EXPLICIT SOLUTIONS AND COEFFICIENT OF RESTITUTION FOR AN ELASTIC ROD WITH VISCOUS DAMPING

By

Feifei Wang and Scott W. Hansen

IMA Preprint Series #2473

(August 2016)

INSTITUTE FOR MATHEMATICS AND ITS APPLICATIONS
UNIVERSITY OF MINNESOTA
400 Lind Hall
207 Church Street S.E.
Minneapolis, Minnesota 55455-0436
Phone: 612-624-6066 Fax: 612-626-7370
URL: http://www.ima.umn.edu

Explicit solutions and coefficient of restitution for an elastic rod with viscous damping

Feifei Wang
Department of Mathematics, Iowa State University
Ames, Iowa 50011
wangff@iastate.edu

Scott W. Hansen
Department of Mathematics, Iowa State University
Ames, Iowa 50011
shansen@iastate.edu

Key words: Signorini problem, elastic rod, coefficient of restitution, viscous wave equation

Abstract

A damped one-dimensional wave equation is used to model an elastic rod that bounces off the ground with a given initial velocity, under the influence of gravity. An explicit solution is derived, based on the Method of Descent and D'Alembert's formula. The time of contact with the ground is determined in terms of the initial velocity, damping coefficient and gravitational constant. We obtain expressions for the motion of the center of mass for the duration of the impact and are able to determine the internal vibrational energy present at the end of the contact time. A corresponding definition of a "coefficient of restitution" is proposed and analyzed.

1 Introduction

The classical problem of determining the height of rebound of a bouncing object has been investigated in a huge number of works going back Newton (1687) who defined the *coefficient of restitution* (COR) as a ratio of relative velocities after and before a collision, Hertz, 1882 [5], who developed the foundations of contact mechanics (see e.g., [8]) based on stresses in spherical elastic bodies, and Love 1905 [12] who investigated the dynamics of colliding elastic rods governed by one-dimensional wave equations.

Although there are numerous applications where impact problems are studied; e.g., sports science, robotics and earthquake dynamics (see e.g., [4], [6], [11], [18], [20], [19], [21], [10]), there are very few situations where a precise knowledge of motion during the impact has been determined. Consequently in most applications, an impact is modeled using a COR. While this methodology has become quite developed, (see e.g., Stronge [17] for a detailed description of various theories of COR and application), there are numerous drawbacks and inconsistencies with this approach, some of which are described in [16].

A COR less than 1 describes an inelastic collision, and hence describes some amount of dissipation (at least in terms of velocity) that occurs during the impact. It has long been thought [16] that dissipation during an impact results from 1) localized plastic deformation; 2) viscous damping in the material; and 3) energy transfer to vibrational energy. Therefore a better knowledge (even in specialized situations) of the portion of translational kinetic energy that is transferred to vibrational energy during the impact, could improve how the COR approach is applied.

One situation where it is possible to write down an explicit solution formula (see e.g., Love [12]) for an impact is the one-dimensional elastic rod

$$\rho v_{tt} - \sigma v_{xx} = f. \tag{1.1}$$

In the above, $u(x,t)$ is the longitudinal displacement at position x and time t; f is an external applied force, ρ is the linear density, and σ is the longitudinal elastic modulus.

The main motivation of this paper is to determine for an elastic rod, possibly a viscous damping term as in (1.2) below, the proportion of vibrational energy in the elastic rod at the end of the impact.

Some results in this direction were obtained by P. Shi [14] who considered the impact of an elastic rod dropped from a specific height to a rigid foundation, and determined the time of impact and rebound velocity of the bottom of the rod. He also obtained a formula for a COR based on the change in velocity of the bottom of the rod.

Here we consider the following constant coefficient elastic rod with viscous damping:

$$v_{tt} + 2rv_t - c^2 v_{xx} \quad = \quad -g \qquad x \in \Omega_L := (0,L),\ t \in (0,+\infty), \tag{1.2}$$

where in comparison to (1.1), we have divided the equation by ρ so that $g \geq 0$ is proportional to the gravitational constant, and the wave speed $c = \sqrt{\frac{\sigma}{\rho}}$ is positive. The viscous damping term $2rv_t$ $(r \geq 0)$ describes a frictional force proportional to the velocity.

The rod is assumed to be stress-free at the end $x = L$ and we impose Signorini boundary conditions at the end $x = 0$:

$$\begin{aligned} v_x(L,t) &= 0, \qquad t \in (0,+\infty), && (1.3)\\ v_x(0,t) &\leq 0, \qquad t \in (0,+\infty), && (1.4)\\ v(0,t) &\geq 0, \qquad t \in (0,+\infty), && (1.5)\\ v(0,t)v_x(0,t) &= 0, \qquad t \in (0,+\infty). && (1.6) \end{aligned}$$

In our formulation of this problem, we assume that the rod impacts the ground at time 0 with constant initial velocity $-\mu$:

$$\begin{aligned} v(x,0) &= 0, \qquad x \in \Omega_L, && (1.7)\\ v_t(x,0) &= -\mu, \qquad x \in \Omega_L, && (1.8) \end{aligned}$$

and with zero displacement from the reference configuration

$$X(x,0) = x, \qquad x \in [0,L],$$

thus the deformed position at time t is given by

$$X(x,t) = x + v(x,t). \tag{1.9}$$

The Signorini boundary conditions (1.4)–(1.6) (also called unilateral constraints) essentially state that the bottom of the rod should be stress-free while not in contact with the ground and the Dirichlet condition $v(0,t) = 0$ should be imposed when in contact with the ground.

Signorini problems have been considered in a wide variety of contact problems for plates plates, beams, strings etc., see e.g., [2], [15], [1], and can be expressed as a variational inequality, for which there is a corresponding definition of a weak solution. For the damped problem (1.2)–(1.6), but with general initial conditions of finite energy, Rivera and Oquendo [13] proved global existence of weak solutions and obtained asymptotic decay results. Lebeau and Schatzman [9] studied an analogous multidimensional undamped wave equation on a half space, and proved existence and uniqueness of solutions in a suitably defined functions space. Controllability in the context of a string equation was considered in [3].

For the present paper, we only need to consider the time interval $[0, t_b + \epsilon)$, where $[0, t_b]$ is the contact interval and ϵ is sufficiently small so that there is at most one bounce. In this situation, solutions are classical except for jumps in the derivatives along certain characteristic rays due to the bounce. Here t_b (possibly $= \infty$) is defined by

$$t_b = \sup\{t > 0 : v(0, \tau) = 0, \quad 0 \leq \tau < t\}. \tag{1.10}$$

Based on the Method of Descent and D'Alembert's formula, we obtain explicit solution formulas for $v(x,t)$ over the contact interval $[0, t_b]$. The contact time t_b is determined in terms of a computable formula in Theorem 1. In particular, we show $t_b \geq t_1 := 2L/c$. In the case $r = 0$, an explicit formula in terms of parameters μ, L, c, and g for t_b is derived, which in particular shows that $t_1 \leq t_b \leq 2t_1$. We also find expressions for the motion of the center of mass over the time interval $[0, t_b + \epsilon]$ for small ϵ. At the time t_b, the energy of the elastic rod has an orthogonal decomposition into *translational energy*, corresponding to the motion of the center of mass and and *vibrational energy*, corresponding to energy of vibrations. We are able to calculate this decomposition at the time of impact, and define an associated COR based on the ratio of translational energy after and before the collision. Based on this definition of COR, we are able to make some observations about the dependence of internal vibrational energy as a function of the μ, the velocity of impact; see Section 4.

2 Explicit integral representation of solution

During the time interval $[0, t_b]$, (1.2)–(1.8) can be written as:

$$\begin{cases} v_{tt} + 2rv_t - c^2 v_{xx} = -g, & (x,t) \in \Omega_L \times (0, t_b), \\ v(x,0) = 0, \ v_t(x,0) = -\mu, & x \in \Omega_L, \\ v(0,t) = 0, \ v_x(L,t) = 0, & t \in (0, t_b). \end{cases} \tag{2.11}$$

It is easy to see that solutions of (2.11) coincide with solutions $\hat{v}$ of

$$\begin{cases} \hat{v}_{tt} + 2r\hat{v}_t - c^2 \hat{v}_{xx} = -g, & (x,t) \in \Omega_{2L} \times (0, t_b), \\ \hat{v}(x,0) = 0, \ \hat{v}_t(x,0) = -\mu, & x \in \Omega_{2L}, \\ \hat{v}(0,t) = 0, \ \hat{v}(2L,t) = 0, & t \in (0, t_b). \end{cases} \tag{2.12}$$

Setting $\hat{v}(x,t) = e^{-rt}w(x,t)$ in (2.12) results in

$$\begin{cases} w_{tt} - c^2 w_{xx} = r^2 w - g e^{rt}, & (x,t) \in \Omega_{2L} \times (0,t_b), \\ w(x,0) = 0, \ w_t(x,0) = -\mu, & x \in \Omega_{2L}, \\ w(0,t) = 0, \ w(2L,t) = 0, & t \in (0,t_b). \end{cases} \tag{2.13}$$

We see below that (2.11) can be solved explicitly using the method of descent together with the reflection principle. For a first step, consider the homogeneous problem on the infinite domain:

$$\begin{cases} u_{tt} - c^2 u_{xx} - c^2\lambda^2 u = 0, & x \in \mathbb{R}, \quad t \in (0,+\infty), \\ u(x,0) = 0, \ u_t(x,0) = \varphi(x). & x \in \mathbb{R}. \end{cases} \tag{2.14}$$

Lemma 1. *Assume φ is C^2 on $\mathbb{R}$. Then the classical solution to (2.14) is given by*

$$u(x,t) = \frac{1}{2c}\int_{x-ct}^{x+ct} I_0(\lambda s)\varphi(y)\,dy, \tag{2.15}$$

where $s = \sqrt{c^2t^2 - (x-y)^2}$ and

$$I_0(z) = \frac{2}{\pi}\int_0^{\pi/2} \cosh(z\sin\theta)\,d\theta, \tag{2.16}$$

is the modified Bessel function of the second kind.

Proof: We apply the "method of descent"; see e.g., [7]. Let u be the solution of (2.14) and define $\hat{u}(x_1,x_2,t) = \cosh(\lambda x_2)u(x_1,t)$. Then it is easy to verify that

$$\begin{cases} \hat{u}_{tt} - c^2(\hat{u}_{x_1x_1} + \hat{u}_{x_2x_2}) = 0 & x_1,x_2 \in \mathbb{R}, t \in (0,+\infty), \\ \hat{u}(x_1,x_2,0) = 0, \ \hat{u}_t(x_1,x_2,0) = \cosh(\lambda x_2)\varphi(x_1), & x_1,x_2 \in \mathbb{R}. \end{cases} \tag{2.17}$$

On the other hand $\hat{u}$ is also given by the spherical means formula

$$\hat{u}(x_1,x_2,t) = \frac{1}{2\pi c}\iint_{r<ct} \frac{\cosh(\lambda y_2)\varphi(y_1)}{\sqrt{c^2t^2 - r^2}}\,dy_1\,dy_2,$$

where $r^2 = (y_1-x_1)^2 + (y_2-x_2)^2$. It follows that

$$\begin{aligned} u(x_1,t) &= \hat{u}(x_1,0,t) \\ &= \frac{1}{2\pi c}\int_{x_1-ct}^{x_1+ct}\int_{-\sqrt{c^2t^2-(y_1-x_1)^2}}^{\sqrt{c^2t^2-(y_1-x_1)^2}} \frac{\varphi(y_1)\cosh(\lambda y_2)}{\sqrt{c^2t^2-(y_1-x_1)^2-y_2^2}}\,dy_2\,dy_1 \\ &= \frac{1}{2\pi c}\int_{x_1-ct}^{x_1+ct}\varphi(y_1)\int_{-s}^{s}\frac{\cosh(\lambda y_2)}{\sqrt{s^2-y_2^2}}\,dy_2\,dy_1; \qquad (s = \sqrt{c^2t^2-(y_1-x_1)^2}) \\ &= \frac{1}{2\pi c}\int_{x_1-ct}^{x_1+ct}\varphi(y_1)\int_{-\pi/2}^{\pi/2}\cosh(\lambda s\sin\theta)\,d\theta\,dy_1 \\ &= \frac{1}{2c}\int_{x_1-ct}^{x_1+ct}\varphi(y_1)I_0(\lambda s)\,dy_1, \end{aligned}$$

as claimed. The proof is complete.

For the moment, consider problem (2.13) in the more general form:

$$\begin{cases} u_{tt} - c^2 u_{xx} - r^2 u = h(x,t), & x \in \Omega_{2L},\ t \in (0,+\infty), \\ u(x,0) = 0,\ u_t(x,0) = \varphi(x), & x \in \Omega_{2L}, \\ u(0,t) = u(2L,t) = 0 & t \in (0,+\infty). \end{cases} \tag{2.18}$$

We will use symmetry to extend the data in (2.18) to all of $\mathbb{R}$. To this end, given a function $f : (0,2L) \to \mathbb{R}$, let $\tilde{f} : (-2L,2L) \setminus \{0\} \to \mathbb{R}$ be the odd extension of f. Then define the *symmetric extension* $f^e : \mathbb{R} \setminus 2L\mathbb{Z} \to \mathbb{R}$ as the periodic extension of $\tilde{f}$.

Proposition 1. *Assume that $\varphi \in C[0,2L]$, h and $h_t \in C([0,2L] \times [0,T])$. Then (2.18) has a unique weak solution u in $C([0,T]; H_0^1[0,2L])$, and u_t in $C([0,T]; L^2(0,2L))$, which is given pointwise by*

$$\begin{aligned} u(x,t) &= \frac{1}{2c}\int_{x-ct}^{x+ct} I_0(r\sqrt{t^2-(x-y)^2/c^2})\varphi^e(y)\,dy \\ &\quad + \frac{1}{2c}\int_0^t \int_{x-c\tau}^{x+c\tau} I_0(r\sqrt{(\tau^2-(x-y)^2/c^2})h^e(y,t-\tau)\,dy\,d\tau. \end{aligned} \tag{2.19}$$

The solution above is continuous and continuously differentiable except on the characteristics $ct = \pm(x-2kL)$, $k \in \mathbb{Z}$, where the partial derivatives u_x and u_t could have jump discontinuities.

Proof: Under the assumptions on φ and h, it is well known that (2.18) has a unique weak solution as described in Proposition 1. Let u_1 denote solution to the problem (2.18) with $h = 0$. It is easily verified that the reflection principal applies to formula (2.15) and problem (2.14) exactly the same way that D'Alembert's formula applies to the undamped ($r = 0$) wave equation (2.18). Hence by the reflection principle u_1 coincides with the solution u_1^e of the problem (2.14) with initial velocity φ^e (and $h \equiv 0$). Thus

$$u_1(x,t) = \frac{1}{2c}\int_{x-ct}^{x+ct} I_0(r\sqrt{t^2-(x-y)^2/c^2})\varphi^e(y)\,dy. \tag{2.20}$$

On the other hand, by Duhamel's principle the solution u_2 of (2.18) with $\varphi = 0$ is

$$\begin{aligned} u_2(x,t) &= \frac{1}{2c}\int_0^t \int_{x-c(t-\tau)}^{x+c(t-\tau)} I_0(r\sqrt{(t-\tau)^2-(x-y)^2/c^2})h^e(y,\tau)\,dy\,d\tau \\ &= \frac{1}{2c}\int_0^t \int_{x-c\tau}^{x+c\tau} I_0(r\sqrt{(\tau)^2-(x-y)^2/c^2})h^e(y,t-\tau)\,dy\,d\tau. \end{aligned} \tag{2.21}$$

The solution u is the superposition of u_1, u_2.

From the solution formula, it is clear that u is continuous for all x and t and the first derivatives u_x, u_t are piecewise continuous with possible discontinuities along the characteristics $ct = \pm(x-2kL)$, $k \in \mathbb{Z}$. This completes the proof.

2.1 Calculation of jumps along characteristics

Let $u(x,t)$ be the solution of (2.18) as given by (2.19) with $\lambda = r/c$. A calculation gives

$$
\begin{aligned}
u_x(x,t) = \quad & \frac{1}{2c}(\varphi^e(x+ct) - \varphi^e(x-ct)) \\
& -\frac{1}{2c}\int_{x-ct}^{x+ct} I_1(\lambda s(t,x-y))\frac{(x-y)\lambda}{s(t,x-y)}\varphi^e(y)\,dy \\
& +\frac{1}{2c}\int_0^t (h^e(x+c\tau,t-\tau) - h^e(x-c\tau,t-\tau))\,d\tau \\
& +\frac{1}{2c}\int_0^t\int_{x-c\tau}^{x+c\tau}\lambda I_1(\lambda s(\tau,x-y))\frac{-(x-y)}{s(\tau,x-y)}h^e(y,t-\tau)\,dy\,d\tau, \qquad (2.22)
\end{aligned}
$$

where $s(t,r) = \sqrt{c^2t^2 - r^2}$, and

$$
I_1(z) = I_0'(z) = \frac{1}{\pi}\int_0^\pi \cos\theta e^{z\cos\theta}\,d\theta
$$

is the first order modified Bessel function.

Let $\Xi^\pm$ denote the set of points (x,t) that are on the characteristics $ct = \pm(x - x_0)$ emanating from points $(x_0, 0)$ with $x_0 \in 2L\mathbb{Z}$, and let $\Xi = \Xi^+ \cup \Xi^-$. If φ is continuous on $(0, 2L)$ but φ^e has jump discontinuities, then (2.22) remains valid for points $(x,t) \notin \Xi$. Let $[\psi(x)] = \psi(x^+) - \psi(x^-)$ denote the jump of function ψ at x. For functions $\beta(x,t)$ with jump discontinuities on the characteristics Ξ, define $[\beta(x,t)]$ to be the jump of β at (x,t), as a function of t, with x fixed.

Consider the case where $(x,t) = (x_0 - ct, t) \in \Xi^- \setminus \Xi^+$. Since the only contributions to $[u_x(x,t)]$ are due to terms in the first line of (2.22), we have

$$
[u_x(x,t)] = [u_x(x_0 - ct, t)] = \frac{1}{2c}([\varphi^e(x_0)] - [\varphi^e(x_0 - 2ct)]) = \frac{1}{2c}[\varphi^e(x_0)].
$$

If instead, $(x,t) = (x_0 + ct, t) \in \Xi^+ \setminus \Xi^-$, noting that along these characteristics, crossing a characteristic in the t direction corresponds to the negative jump in the x direction. Hence

$$
[u_x(x,t)] = [u_x(x_0 + ct, t)] = \frac{-1}{2c}([\varphi^e(2ct + x_0)] - [\varphi^e(x_0)]) = \frac{1}{2c}[\varphi^e(x_0)].
$$

Similarly,

$$
\begin{aligned}
u_t(x,t) \quad = \quad & \frac{1}{2}(\varphi^e(x+ct) + \varphi^e(x-ct)) \\
& +\frac{1}{2}\int_{x-ct}^{x+ct}\frac{rtI_1(\lambda s(t,x-y))}{s(t,x-y)}\varphi^e(y)\,dy \\
& +\frac{1}{2c}\int_{x-ct}^{x+ct} I_0(\lambda s(t,x-y))h^e(y,0)\,dy \\
& +\frac{1}{2c}\int_0^t\int_{x-c\tau}^{x+c\tau} I_0(\lambda s(\tau,x-y))h_t^e(y,t-\tau)\,dy\,d\tau \qquad (2.23)
\end{aligned}
$$

We again can easily calculate $[u_t]$, the jump in u_t along the characteristics. If $(x,t) \in \Xi^- \setminus \Xi^+$, then

$$[u_t(x,t)] = [u_t(x_0 - ct, t)] = \frac{1}{2}([\varphi^e(x_0 - 2ct)] + [\varphi^e(x_0)]) = \frac{1}{2}[\varphi^e(x_0)].$$

If $(x,t) \in \Xi^+ \setminus \Xi^-$, then

$$[u_t(x,t)] = [u_t(x_0 + ct, t)] = \frac{-1}{2}([\varphi^e(x_0)] + [\varphi^e(x_0 + 2ct)]) = -\frac{1}{2}[\varphi^e(x_0)].$$

We summarize this calculation in the following.

Proposition 2. *The solutions $u(x,t)$ given in Proposition 1 satisfy the following properties:*
(i) If $(x,t) = (x_0 - ct, t) \in \Xi^- \setminus \Xi^+$, then

$$[u_x(x,t)] = \frac{1}{2c}[\varphi^e(x_0)], \qquad [u_t(x,t)] = \frac{1}{2}[\varphi^e(x_0)].$$

(ii)If $(x,t) = (x_0 + ct, t) \in \Xi^+ \setminus \Xi^-$, then

$$[u_x(x,t)] = \frac{1}{2c}[\varphi^e(x_0)], \qquad [u_t(x,t)] = -\frac{1}{2}[\varphi^e(x_0)].$$

(iii) If $(x,t) = (x_0 + ct, t) = (x_1 - ct, t) \in \Xi^+ \cap \Xi^-$, then

$$[u_x(x,t)] = \frac{[\varphi^e(x_0)] + [\varphi^e(x_1)]}{2c}, \qquad [u_t(x,t)] = \frac{[\varphi^e(x_1)] - [\varphi^e(x_0)]}{2}.$$

2.2 Calculation of contact time

In the case of interest, namely $\varphi(x) = -\mu$ is a constant and $h(x,t) = -ge^{rt}$ with $x \in \Omega_{2L}$. Therefore $\varphi^e(x) = -\mu(x)^e$ and $h(x,t)^e = -g(x)^e e^{rt}$, where $g(x)^e$ and $\mu(x)^e$ denote the symmetric extensions defined on $\mathbb{R} \setminus 2L\mathbb{Z}$ of the constant functions g, μ (originally defined on $(0, 2L)$). With $\lambda = \frac{r}{c}$, we see from (2.13) and Proposition 1 that the solution to the original problem (2.11) is

$$\begin{aligned} v(x,t) &= e^{-rt}u(x,t) = e^{-rt}w(x,t), \quad \text{where} \qquad (2.24) \\ w(x,t) &= \frac{1}{2c}\int_{x-ct}^{x+ct} I_0(\lambda s(t,(x-y))(-\mu^e(y))\,dy; \quad (s(t,r) := \sqrt{c^2t^2 - r^2}), \\ &+ \frac{1}{2c}\int_0^t \int_{x-c\tau}^{x+c\tau} I_0(\lambda s(\tau, x-y))(-g^e(y)e^{r(t-\tau)})\,dy\,d\tau. \end{aligned}$$

Since $v_x(0,t) = e^{-rt}w_x(0,t)$, the boundary condition (1.4) holds if and only if $w_x(0,t) \leqslant 0$. Therefore, we compute $w_x(0,t) = u_x(0,t)$ where $u(x,t)$ is given by (2.19) with $\varphi^e = -\mu^e$ and $h^e = -g^e e^{rt}$. We obtain

$$\begin{aligned} w_x(0,t) &= \frac{1}{2c}(\varphi^e(ct) - \varphi^e(-ct)) \\ &-\frac{1}{2c}\int_{-ct}^{ct} I_1(\lambda s(t,y))\frac{(-y)\lambda}{s(t,y)}\varphi^e(y)\,dy \\ &+\frac{1}{2c}\int_0^t h^e(c\tau, t-\tau) - h^e(-c\tau, t-\tau)\,d\tau \\ &+\frac{1}{2c}\int_0^t \int_{-c\tau}^{c\tau} \lambda I_1(\lambda s(\tau,y))\frac{y}{s(\tau,y)}h^e(y, t-\tau)\,dy\,d\tau. \qquad (2.25) \end{aligned}$$

Assume for some $k = k(t) \in \mathbb{N}_0 = \{0, 1, 2...\}$ that

$$2Lk < ct < 2L(k+1),$$

or equivalently

$$t_1 k < t < t_1(k+1). \tag{2.26}$$

Using that (i) $s(t,r)$ is even with respect to r, (ii) $\phi^e = -\mu^e$ is an odd function that is constant on $(2jL, 2(j+1)L), \forall j \in \mathbb{Z}$, (iii) $s(t, \pm ct) = 0$, (iv) $\lambda = r/c$, we compute the first two terms in (2.25),

$$\begin{aligned}
& \frac{1}{2c}(\varphi^e(ct) - \varphi^e(-ct)) - \frac{1}{2c}\int_{-ct}^{ct} I_1(\lambda s(t,y))\frac{(-y)\lambda}{s(t,y)}\varphi^e(y)\,dy \\
= \; & \frac{1}{2c}(2\varphi^e(ct)) - \frac{1}{2c}\int_{-ct}^{ct}\left(\frac{d}{dy}I_0(\lambda s(t,y))\right)\varphi^e(y)\,dy \\
= \; & \frac{\varphi^e(ct)}{c} - \frac{1}{2c}\sum_{j=-k}^{k-1}\int_{2Lj}^{2L(j+1)}\left(\frac{d}{dy}I_0(\lambda s(t,y))\right)\phi^e(y)\,dy \\
& -\frac{1}{2c}\left(\int_{-ct}^{-2Lk} + \int_{2Lk}^{ct}\right)\left(\frac{d}{dy}I_0(\lambda s(t,y))\right)\phi^e(y)\,dy \\
= \; & \frac{\varphi^e(ct)}{c} - \frac{1}{2c}\{\sum_{j=-k}^{k-1}\left(I_0(\lambda s(t,y))\phi^e(y)\,\Big|_{2Lj}^{2L(j+1)}\right) + I_0(\lambda s(t,y))\phi^e(y)\,\Big|_{-ct}^{-2Lk} \\
& +I_0(\lambda s(t,y))\phi^e(y)\,\Big|_{2Lk}^{ct}\} \\
= \; & \frac{1}{2c}2\varphi^e(0^+)\{I_0(\lambda s(t,0)) - (\;I_0(\lambda s(t,2L)) + I_0(\lambda s(t,-2L))\;) \\
& +(\;I_0(\lambda s(t,4L)) + I_0(\lambda s(t,-4L))\;) - ...... + (-1)^k\,(I_0(\lambda s(t,2kL)) + I_0(\lambda s(t,-2kL)))\} \\
= \; & \begin{cases} \frac{1}{2c}\left(2\varphi^e(0^+)I_0(rt)\right) & k = 0, \\ \frac{1}{2c}\left(2\varphi^e(0^+)\left(I_0(rt) + 2\sum_{j=1}^{k}(-1)^j I_0(r\sqrt{t^2-(jt_1)^2})\right)\right) & k \geqslant 1. \end{cases} \\
= \; & \frac{-\mu}{c}H_r(t),
\end{aligned} \tag{2.27}$$

where on each interval $t \in (t_1 k, t_1(k+1))$,

$$H_r(t) := \begin{cases} I_0(rt), & t \in (0, t_1 := \frac{2L}{c}), \\ I_0(rt) + 2\sum_{j=1}^{k}(-1)^j I_0(r\sqrt{t^2-(jt_1)^2}) & t \in (kt_1, (k+1)t_1). \end{cases}$$

and k is defined in terms of t as in (2.26). Similar calculations can be used to simplify the last two terms in (2.25). Hence we obtain

$$w_x(0,t) = \Psi_r(t) := \frac{-\mu}{c}H_r(t) - \frac{g}{c}\int_0^t e^{r(t-\tau)}H_r(\tau)d\tau. \tag{2.28}$$

Returning to the original system (1.2)–(1.8), we see that inequality (1.4) is maintained if and only if $\Psi_r(t) \leqslant 0$. Therefore, we have the following result that defines time t_b of the first bounce in equation (1.10).

Theorem 1. *Let set $S = \{t : \Psi_r(t) > 0\}$, where $\Psi_r(t)$ is defined by (2.28).*
(i) If $S = \emptyset$, there is no bounce.

(ii) If $S \neq \emptyset$, then the first bounce is given by $t_b = \inf S \geqslant t_1 = 2L/c$.
(iii) $t_b = t_1$ if and only if $\Psi_r(t_1^-) + 2\mu/c > 0$, i.e.

$$-\mu I_0(rt_1) + 2\mu - g \int_0^{t_1} e^{r(t_1-\tau)} I_0(r\tau)\, d\tau > 0, \tag{2.29}$$

Proof. Part (i) is clear. Hence assume S is not empty, and $t_b \in \mathbb{R}$. Note that $\Psi_r(0) < 0$ and is strictly decreasing for $t \in (0, t_1)$. Therefore $t_b \geqslant t_1$, which proves part (ii). For part (iii), in order for a bounce to occur at time t_1, the stress function $\Psi_r(t)$ has to change sign at time t_1. By Proposition 2, $[u_x(0, t_1)] = 2\mu/c$. Hence, the condition for a bounce is $\Psi_r(t_1^-) + 2\mu/c > 0$, which simplifies to (2.29). $\square$

We examine the condition (2.29) in more details below:

General case $r \neq 0$ and $g \neq 0$: The condition (2.29) simplifies to

$$\mu(2 - I_0(rt_1)) > g \int_0^{t_1} e^{r(t_1-\tau)} I_0(r\tau)\, d\tau. \tag{2.30}$$

Since the right hand side is positive, a necessary condition for solving (2.30) is

$$2 - I_0(rt_1) > 0.$$

Since the graph of $I_0(z)$ is monotonically increasing for $z \geqslant 0$, the above condition is equivalent to

$$rt_1 < I_0^{-1}(2) \simeq 1.8. \tag{2.31}$$

Then (2.30) can be simplified as

$$\mu/g > \frac{\int_0^{t_1} e^{r(t_1-\tau)} I_0(r\tau)\, d\tau}{2 - I_0(rt_1)}. \tag{2.32}$$

Therefore, in order for a bounce to occur at time t_1, r must be sufficiently small so that (2.31) holds. If also μ/g is large enough such that (2.32) holds, then there will be a bounce at time t_1.

We examine in further details for two special cases.

The case $r = 0$ and $g > 0$: To apply Theorem 1, in case of $r = 0$, we know that the stress function $\Psi_r(t)$ becomes

$$\Psi_0(t) = -\frac{\mu}{c} H_0(t) - \frac{g}{c} \int_0^t H_0(\tau)\, d\tau,$$

where

$$H_0(t) := \begin{cases} 1, & t \in (0, t_1), \\ 1 + 2\sum_{j=1}^{k} (-1)^j & t \in (kt_1, (k+1)t_1). \end{cases}$$

Set S in Theorem 1 is defined by t for which $\Psi_0(t) > 0$.

The function $\Psi_0(t)$ is piecewise linear and $2t_1$-periodic. One easily deduces the following, which is more precise than Theorem 1.

Corollary 1. *Assume $r = 0$ and $g > 0$ and $\mu > 0$. There is a first bounce at time $t_b \geqslant t_1$ for which*
(i) if $\mu \geqslant gt_1$, the first bounce time is $t_b = t_1$
(ii) $0 < \mu < gt_1$, the first bounce time is $t_b = 2t_1 - \frac{\mu}{g}$.

Remark 1. *If $r = 0$, $g = 0$, then $t_1 = t_b$ for all $\mu > 0$, since hypothesis in (ii) is vacuous and only (i) applies.*

We mention that Corollary 1 was also obtained in [14], although his formulation is different than ours.

The case $g = 0, r \geqslant 0$: The condition (2.29) for a bounce at time $t_b = t_1 = 2L/c$ reduces to

$$I_0(rt_1) < 2;$$

or equivalently,

$$rt_1 < I_0^{-1}(2) \simeq 1.8. \tag{2.33}$$

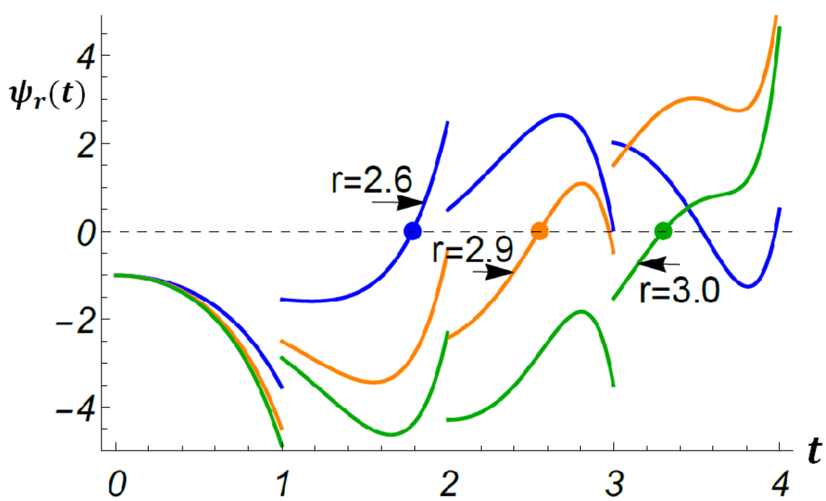

Figure 1: Plot for $\Psi_r(t)$ with different r values of 2.6, 2.9 and 3.0, when $g = 0, t_1 = 1, \mu = 1$, and $c = 1$, the time t_b of first bounce for each case is indicated by a dot.

Hence for $0 \leqslant r \leqslant I_0^{-1}(2)/t_1$, we have $t_b = t_1 = 2L/c$. Mathematica computations indicate that for slightly larger values r, the bounce can occur at later times. Figure 1 shows a plot of the function $\Psi_r(t)$ on the interval $(0, 4t_1)$ in the case when $g = 0, t_1 = 1, \mu = 1, c = 1$, with values of r varying as 2.6, 2.9 and 3.0. For each case, the bounce time t_b occurs when the graph of $\Psi_r(t)$ crosses the t-axis. The graph indicates the bounce time t_b at various positions within the interval $(t_1, 2t_1)$, $(2t_1, 3t_1)$ and $(3t_1, 4t_1)$.

3 Momentum, Center of Mass and Energy

First we derive formulas for the center of mass and momentum of the rod.

3.1 Momentum and Center of Mass

We consider the system (2.11). The momentum of the rod for $t \geqslant 0$ is given by

$$P(t) = \int_0^L v_t(x,t)\,dx. \tag{3.34}$$

Integration of both sides of equation (2.11) with respect to x on $[0, t_b]$ results in

$$\begin{aligned} P'(t) + 2rP(t) &= \int_0^L c^2 v_{xx}(x,t) - g\,dx && (3.35)\\ &= -c^2 v_x(0,t) - gL && (3.36)\end{aligned}$$

Therefore since $P(0) = \int_0^L (-\mu)\,dx = -\mu L$ and $v_x(0,t) = e^{-rt}\Psi_r(t)$, where $\Psi_r(t)$ is defined in (2.28), P satisfies

$$P'(t) + 2rP(t) = -c^2 e^{-rt}\Psi_r(t) - gL, \quad 0 \leqslant t \leqslant t_b; \quad P(0) = -\mu L. \tag{3.37}$$

We solve the ODE on $[0, t_b]$ and get

$$P(t) = -c^2 e^{-2rt} \int_0^t e^{r\tau}\Psi_r(\tau)\,d\tau - \frac{gL}{2r}(1 - e^{-2rt}) - \mu L e^{-2rt}. \tag{3.38}$$

Let $h(t)$ denote the position at time t of center of mass of the rod relative to the midpoint of the rod at time 0. Thus $h(0) = 0$. For any $t \geqslant 0$, $h(t) = \frac{1}{L}\int_0^L X(x,t)\,dx - L/2$, where $X(x,t)$ denotes the position of the point with reference position x at time t defined in (1.9). Then $h(t)$ is given by

$$\begin{aligned} h(t) &= \frac{1}{L}\int_0^L X(x,t)\,dx - L/2 = \frac{1}{L}\int_0^L v(x,t)\,dx \\ &= \frac{1}{L}\int_0^L \left(v(x,0) + \int_0^t v_t(x,\tau)\,d\tau \right) dx \\ &= \frac{1}{L}\int_0^t \int_0^L v_t(x,\tau)\,dx\,d\tau \\ &= \frac{1}{L}\int_0^t P(\tau)\,d\tau. && (3.39)\end{aligned}$$

Define

$$v^0(x) = \lim_{t\to t_b^-} v(x,t), \qquad v^1(x) = \lim_{t\to t_b^-} v_t(x,t).$$

These limits exist since by Proposition 1, $v(x,t_b)$ is continuous and $v_t(x,t_b)$ is piecewise continuous for $0 < x < L$. Let

$$\begin{aligned} h^0 &= h(t_b) = \frac{1}{L}\int_0^L v^0(x)\,dx = \frac{1}{L}\int_0^{t_b} P(\tau)\,d\tau, && (3.40)\\ h^1 &= h'(t_b) = \frac{1}{L}\int_0^L v^1(x)\,dx = \frac{1}{L}P(t_b). && (3.41)\end{aligned}$$

Note that $v^0(x)$ and $v^1(x)$ do not need to be known in order to compute h^0 and h^1 since $P(t)$ is given explicitly by equation (3.38).

Let $t_2 = \sup\{t : v(0,t) > 0 \text{ on } (t_b, t)\}$. We can also solve $h(t)$ and $P(t)$ on time interval (t_b, t_2). The PDE on this interval is:

$$\begin{cases} v_{tt} + 2rv_t - c^2 v_{xx} = -g, & (x,t) \in \Omega_L \times (t_b, t_2), \\ v(x,t_1) = v^0(x),\ v_t(x,t_1) = v^1(x), & x \in \Omega_L, \\ v_x(0,t) = v_x(L,t) = 0, & t \in (t_b, t_2). \end{cases} \tag{3.42}$$

Since the bottom of the rod is stress free on this interval, it follows that $\Psi_r(t) = 0$ on (t_1, t_b). Thus (3.35) changes to

$$P'(t) + 2rP(t) = -gL \qquad P(t_b) = Lh^1.$$

Solving this ODE, one obtains

$$P(t) = -\frac{gL}{2r} + (h^1 L + \frac{gL}{2r})e^{-2r(t-t_b)}, \quad t_b \leqslant t \leqslant t_2. \tag{3.43}$$

From (t_b, t_2), using (3.40) and (3.43), $h(t)$ is given by

$$\begin{aligned} h(t) &= h^0 + \frac{1}{L}\int_{t_b}^t P(\tau)\, d\tau \\ &= \frac{A - g(t-t_b) - h^1 e^{-2r(t-t_b)}}{2r} + \frac{g}{(2r)^2}(1 - e^{-2r(t-t_b)}), \end{aligned} \tag{3.44}$$

where $A = h^1 + 2rh^0$. In summary,

$$h(t) = \begin{cases} \frac{1}{L}\int_0^t P(\tau)\, d\tau, & t \in [0, t_b], \\ \frac{A - g(t-t_b) - h^1 e^{-2r(t-t_b)}}{2r} + \frac{g}{(2r)^2}(1 - e^{-2r(t-t_b)}), & t \in [t_b, t_2], \end{cases} \tag{3.45}$$

where

$$P(t) = \begin{cases} -c^2 e^{-2rt}\int_0^t e^{r\tau}\Psi(\tau)\, d\tau - \frac{gL}{2r}(1 - e^{-2rt}) - \mu L e^{-2rt}, & t \in [0, t_b], \\ -\frac{gL}{2r} + (h^1 L + \frac{gL}{2r})e^{-2r(t-t_b)}, & t \in [t_b, t_2], \end{cases} \tag{3.46}$$

and h^0 and h^1 are defined in (3.40) and (3.41).

The case $r = 0$: In the undamped case, the center of mass and momentum can be determined in a more explicit form. We consider the following cases

(i) for $r = 0,\ g \geqslant 0,\ \mu \geqslant gt_1$**, i.e.** $t_b = t_1$:

Since now $\Psi_0(t) = -\frac{\mu}{c} - \frac{g}{c}t$, from (3.38):

$$P(t) = \mu(ct - L) + gt(ct/2 - L),\ t \in [0, t_1]. \tag{3.47}$$

Consequently

$$h(t) = \frac{1}{L}\int_0^t P(\tau)\, d\tau = \frac{1}{L}(gct^3/6 + (\mu c - gL)t^2/2 - \mu L t), \quad t \in [0, t_1]. \tag{3.48}$$

Therefore

$$h^0 = h(t_1) = -\frac{2gL^2}{3c^2}, \quad h^1 = \frac{P(t_1)}{L} = \frac{\mu L}{L} = \mu. \tag{3.49}$$

Thus, in the pure elastic case without damping, the momentum immediately after the collision is the same in magnitude as before the collision. However, when $g > 0$, internal stresses remain present.

For $t \in (t_1, t_2)$: Take limit as $r \to 0^+$ from equation (3.43) and (3.44), one obtains

$$P(t) = \mu L - Lgt + 2L^2 g/c, \; h(t) = -\frac{8gL^2}{3c^2} + \mu t - \frac{gt^2}{2} - \frac{2L(\mu - gt)}{c}.$$

In summary, if $r = 0$, $g \geqslant 0$, $\mu \geqslant gt_1$, then

$$P(t) = \begin{cases} \mu(ct - L) + gt(ct/2 - L), & t \in [0, t_1], \\ \mu L - Lgt + 2L^2 g/c. & t \in [t_1, t_2]. \end{cases} \tag{3.50}$$

and

$$h(t) = \begin{cases} \frac{1}{L}(gct^3/6 + (\mu c - gL)t^2/2 - \mu L t), & t \in [0, t_1], \\ -\frac{8gL^2}{3c^2} + \mu t - \frac{gt^2}{2} - \frac{2L(\mu - gt)}{c}, & t \in [t_1, t_2]. \end{cases} \tag{3.51}$$

(ii) for $r = 0$, $g > 0$, $0 < \mu/g < t_1$, i.e. $t_b > t_1$:

Solving for $P(t)$ on the intervals $[0, t_1]$, $(t_1, t_b]$ and (t_b, t_2) separately using $\Psi_0(t) = -\frac{\mu}{c} - \frac{gt}{c}$, $\Psi_0(t) = \frac{\mu}{c} - \frac{g}{c}(2t_1 - t)$, $\Psi_0(t) \equiv 0$ on each respective interval. One obtains:

$$P(t) = \begin{cases} \mu(ct - L) + gt(ct/2 - L), & t \in [0, t_1], \\ -\frac{4gL^2}{c} + (\mu + gt)(3L - \frac{ct}{2}) - \frac{\mu ct}{2}, & t \in [t_1, t_b], \\ \frac{4gL^2}{c} + \frac{\mu^2 c}{2g} - L(\mu + gt), & t \in [t_b, t_2], \end{cases} \tag{3.52}$$

and

$$h(t) = \begin{cases} -\mu t - \frac{gt^2}{2} + \frac{\mu c t^2}{2L} + \frac{gct^3}{6L}, & t \in [0, t_1], \\ \frac{(4L - ct)(3\mu c(-2L + ct) + g(4L^2 - 5cLt + c^2 t^2))}{6c^2 L}, & t \in [t_1, t_b], \\ \frac{\mu^3 c^3 + (ct - 4L)(3c^2 g \mu^2 - 6cg^2 L\mu) - 3g^3 L(ct - 4L)^2}{6c^2 g^2 L}, & t \in [t_b, t_2]. \end{cases} \tag{3.53}$$

Remark 2. *One can use (3.50)-(3.53) to compute the maximum height $h_{max} = h(t^*)$ by setting $P(t^*) = 0$. One obtains*

$$t^* = \begin{cases} t_b + \frac{1}{2r}\ln(1 + \frac{2rh^1}{g}), & r \neq 0, \quad t^* < t_2, \\ \frac{2gL + \mu c}{cg}, & r = 0, \quad \mu \geqslant gt_1, \\ \frac{8g^2L^2 - 2cgL\mu + c^2\mu^2}{2cg^2 L}, & r = 0, \quad 0 < \mu < gt_1, \end{cases}$$

Therefore, if $g > 0$, and $t^* \in [t_b, t_2]$, one finds

$$h_{max} = h(t^*) = \begin{cases} \frac{h^1 + 2rh^0}{2r} - \frac{g}{4r^2}\ln(1 + \frac{2rh^1}{g}), & r \neq 0, \quad t^* < t_2, \\ \frac{\mu^2}{2g} - \frac{2gL^2}{3c^2}, & r = 0, \quad \mu \geqslant gt_1, \\ \frac{\mu^2(12g^2L^2 - 8cgL\mu + 3c^2\mu^2)}{24g^3L^2}, & r = 0, \quad 0 < \mu < gt_1. \end{cases}$$

3.2 Energy decomposition

The energy of the rod consists of the sum of the kinetic energy, the strain energy and the gravitational potential energy and is given by

$$\mathcal{E}(t) = \frac{1}{2}\int_0^L \left((v_t)^2 + c^2 v_x^2\right)\, dx + Lgh(t), \tag{3.54}$$

for any $t \in (0, t_2)$. At points where $\mathcal{E}$ is differentiable one finds

$$\begin{aligned} \frac{d}{dt}\mathcal{E}(t) &= \int_0^L (v_t v_{tt} + c^2 v_x v_{xt})\, dx + Lgh'(t) \\ &= c^2 v_x v_t|_0^L + \int_0^L v_t(v_{tt} - c^2 v_{xx})\, dx + P(t)g \\ &= \int_0^L v_t(-2rv_t - g)\, dx + P(t)g \\ &= -2r\int_0^L v_t^2\, dx. \end{aligned} \tag{3.55}$$

The boundary value problem satisfied on (t_b, t_2) is (3.42). Due to the stress free boundary conditions in (3.42), for $t \in (t_b, t_2)$, the eigenfunctions corresponding to (3.42) are $\{\cos k\pi x/L\}_{k=0}^{\infty}$. In particular the constant component is orthogonal to all other eigenfunctions. Hence if we decompose the initial data:

$$v^0(x) = \frac{1}{L}\int_0^L v^0(s)\, ds + z^0(x) = h^0 + z^0(x); \qquad \int_0^L z^0(s)\, ds = 0 \tag{3.56}$$

$$v^1(x) = \frac{1}{L}\int_0^L v^1(s)\, ds + z^1(x) = h^1 + z^1(x); \qquad \int_0^L z^1(s)\, ds = 0, \tag{3.57}$$

where h^0 and h^1 are given in (3.40) and (3.41), then the solution $v(x,t)$ of (3.42) on $[t_b, t_2]$ has the orthogonal decomposition

$$v(x,t) = z(x,t) + h(t), \quad t \in [t_b, t_2] \tag{3.58}$$

where the constant component h satisfies

$$\begin{cases} h'' + 2rh' = -g, & t \in (t_b, t_2), \\ h(t_b) = h^0, & h'(t_b) = h^1, \end{cases} \tag{3.59}$$

and z satisfies

$$\begin{cases} z_{tt} + 2rz_t - c^2 z_{xx} = 0, & (x,t) \in \Omega_L \times (t_b, t_2), \\ z(x, t_b) = z^0,\ z_t(x, t_b) = z^1, & x \in \Omega_L, \\ z_x(0,t) = z_x(L,t) = 0, & t \in (t_b, t_2). \end{cases} \tag{3.60}$$

The solution of (3.59) was discussed in the previous subsection.

Due to the orthogonality of the solutions z and h on $L^2(0, L)$, the total energy $\mathcal{E}$ has the decomposition

$$\mathcal{E}(t) = \mathcal{E}_h(t) + \mathcal{E}_z(t), \tag{3.61}$$

where for $t \in [t_b, t_2]$,

$$\mathcal{E}_z(t) = \frac{1}{2}\int_0^L z_t^2 + c^2 z_x^2\, dx \tag{3.62}$$

$$\mathcal{E}_h(t) = \frac{1}{2}\int_0^L (h'(t))^2 dx + Lgh(t) = \frac{1}{2L}P^2(t) + Lgh(t). \tag{3.63}$$

$\mathcal{E}_z(t)$ is the *vibrational energy*, and $\mathcal{E}_h(t)$ is the energy corresponding to the motion of the center of mass, which we refer to as the *translational energy*.

The goal of this subsection is to determine or approximate this decomposition at the time of bounce t_b. From equation (3.55), (3.58), (3.62), and (3.63), these energies have respective decay rates given by (for $t \in [t_b, t_2]$)

$$\frac{d}{dt}\mathcal{E}_h(t) = -2r\int_0^L (h')^2\, dx = -\frac{2r}{L}P(t)^2, \tag{3.64}$$

$$\frac{d}{dt}\mathcal{E}_z(t) = -2r\int_0^L (z_t)^2\, dx. \tag{3.65}$$

Note in particular that when $r = 0$, $\mathcal{E}_h$ and $\mathcal{E}_z$ are conserved on $[t_b, t_2]$.

3.2.1 The undamped case $r = 0$

When $r = 0$, one can use the conservation of energy law on $[0, t_2]$ to obtain

$$\mathcal{E}(t) = \mathcal{E}(0) = \frac{1}{2}\int_0^L (v_t(x,0)^2 + c^2 v_x(x,0)^2)\, dx + Lgh(0) = \frac{\mu^2 L}{2} := \mathcal{E}_{tot}. \tag{3.66}$$

Furthermore, $\mathcal{E}_h(t)$ can be computed with (3.50)-(3.53) and (3.63). Explicitly, one obtains for the case $\mu \geqslant \mu_0$ (thus $t_1 = t_b$), for $t \in [t_1, t_2]$

$$\begin{aligned}
\mathcal{E}_h(t) &= \frac{1}{2L}L^2(-g(t-2L/c)+\mu)^2 + Lgh(t) \\
&= \frac{L}{2}\left(-g(t-\frac{2L}{c})+\mu\right)^2 + Lg(-\frac{8gL^2}{3c^2} + \mu t - \frac{gt^2}{2} - \frac{2L(\mu - gt)}{c}) \\
&= -\frac{2g^2L^3}{3c^2} + \frac{L\mu^2}{2} \\
&= \frac{L}{2}(\mu^2 - \frac{\mu_0^2}{3}) \qquad \left(\mu_0 = \frac{2gL}{c}\right).
\end{aligned} \tag{3.67}$$

Similarly, one can compute for $t \in [0, t_1]$,

$$\begin{aligned}
\mathcal{E}_h(t) &= \frac{(\mu(ct-L)+gt(ct/2-L))^2}{2L} + Lg\frac{gct^3/6 + (\mu c - gL)t^2/2 - \mu L t}{L} \\
&= \frac{12L^2\mu^2 + 3c^2t^2(2\mu+gt)^2 - 8cLt(3\mu^2+3g\mu t+g^2t^2)}{24L}.
\end{aligned}$$

By similar computation, for the case $0 < \mu < \mu_0$ (thus $t_b > t_1$), using (3.52), (3.53) and (3.66), one obtains

$$\mathcal{E}_h(t) = \begin{cases} \frac{12L^2\mu^2+3c^2t^2(2\mu+gt)^2-8cLt(3\mu^2+3g\mu t+g^2t^2)}{24L}, & t \in [0, t_1], \\ \frac{g^2(4L-3ct)(4L-ct)^3+12c^2\mu^2(ct-3L)^2+12cg\mu(ct-4L)^2(ct-2L)}{24c^2L}, & t \in [t_1, t_b], \\ \frac{1}{24}\mu^2(12L - \frac{8c\mu}{g} + \frac{3c^2\mu^2}{g^2L}) = \frac{L\mu^2(3\mu^2-4\mu\mu_0+3\mu_0^2)}{6\mu_0^2}, & t \in [t_b, t_2]. \end{cases} \tag{3.68}$$

Using the energy decomposition (3.61), conservation of energy (3.66), together with previous expressions for $\mathcal{E}_h$, we have the following result.

Theorem 2. *Let $r = 0$ and bounce time t_b as defined in Corollary 1. At time t_b, the internal energy satisfies*

$$\mathcal{E}_z(t_b) = \begin{cases} -\frac{L\mu^3(3\mu-4\mu_0)}{6\mu_0^2}, & 0 < \mu < \mu_0 = 2gL/c, \\ \frac{\mu_0^2 L}{6}, & \mu \geqslant \mu_0. \end{cases} \tag{3.69}$$

Thus,

$$\mathcal{E}_z(t_b)/\mathcal{E}_{tot} = \begin{cases} -\frac{\mu(3\mu-4\mu_0)}{3\mu_0^2}, & 0 < \mu < \mu_0 = 2gL/c, \\ \frac{\mu_0^2}{3\mu^2}, & \mu \geqslant \mu_0. \end{cases} \tag{3.70}$$

A typical graph of $\mathcal{E}_z(t_b)$ as a function of μ is given in Figure 2. Corresponding graphs of $\mathcal{E}_z(t_b)/\mathcal{E}_{tot}$ and $\mathcal{E}_h(t_b)/\mathcal{E}_{tot}$ are given in Figure 3. We note the following observations:

(i) $\mathcal{E}_z(t_b)/\mathcal{E}_{tot}$ as a function of μ is maximized at $\mu = 2\mu_0/3$.

(ii) $\mathcal{E}_z(t_b)/\mathcal{E}_{tot}$ is a continuously differentiable function of μ for $\mu > 0$.

(iii) $\mathcal{E}_z(t)$ is constant with respect to μ for $\mu \geqslant \mu_0$.

(iv) $\lim_{\mu\to\infty} \frac{\mathcal{E}_z(t_b)}{\mathcal{E}_{tot}} = 0$ for $\mu \geqslant \mu_0$.

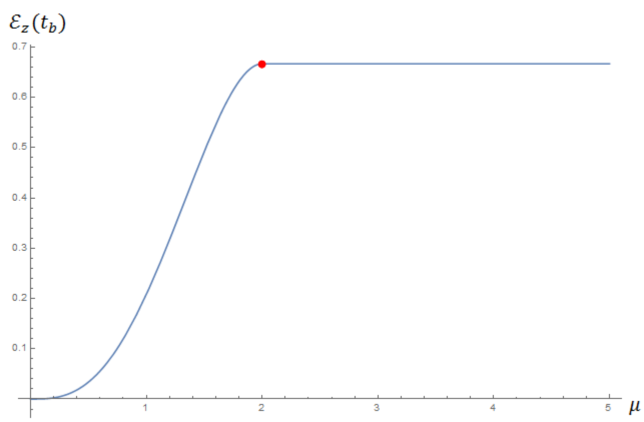

Figure 2: Plot for $\mathcal{E}_z(t_b)$ when $r = 0, c = 1.0,\ L = 1.0,\ g = 1.0$ change with μ, the red dot corresponds to $\mu = \mu_0$.

4 Coefficient of restitution

The standard definition for a coefficient of restitution (COR) for an impact of a particle against a fixed surface normal to the motion of the particle is the ratio of velocities, or equivalently ratio of momenta, immediately after impact (v_1 or P_1) to the immediately before the impact (v_0 or P_0) i.e,

$$e = -\frac{P_1}{P_0} = -\frac{v_1}{v_0}.$$

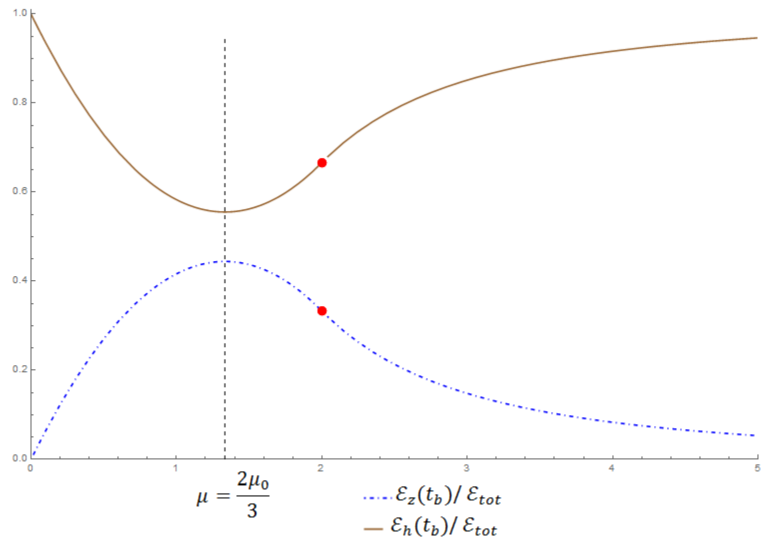

Figure 3: Plot for $\mathcal{E}_h(t_b)/\mathcal{E}(0)$ and $\mathcal{E}_z(t_b)/\mathcal{E}(0)$, when $r = 0, c = 1.0,\ L = 1.0,\ g = 1.0$ change with μ, the red dot corresponds to $\mu = \mu_0$.

Thus a purely elastic collision is described by $e = 1$ and purely inelastic, where the motion of the particle stops at impact is described by $e = 0$. Intermediate values of e describe the degree of inelasticity of the impact. The idea of applying a COR to bouncing objects goes back to Isaac Newton, who suggested (see [17]) for example that glass should have $e = 15/16$ and steel should have $e = 5/9$.

4.1 Momentum coefficient of restitution

Analogously, we can define a momentum coefficient of restitution for the bouncing elastic rod as the ratio of momenta after and before the impact:

$$e_P = -\frac{P(t_b)}{P(0)},$$

where t_b is the bounce time. Equivalently, $e_P = -v_{CM}(t_b)/v_{CM}(0)$, where v_{CM} denotes the velocity of the center of mass.

The undamped case $r = 0$: From equations (3.50)-(3.53), one obtains

$$P(0) = -\mu L, \qquad\qquad P(t_b) = \begin{cases} \mu L, & \mu > gt_1, \\ \frac{c\mu^2}{2g}, & 0 < \mu < gt_1. \end{cases}$$

Thus, we have

$$e_P = \begin{cases} 1, & \mu > gt_1, \\ \frac{\mu c}{2gL} = \frac{\mu}{\mu_0}, & 0 < \mu < gt_1. \end{cases}$$

A flaw in this definition is that when $g > 0$, the position of center of mass at the end of collision is lower than the initial center of mass. Hence, even when $e_P = 1$, the elastic rod will not bounce as high as it was dropped from (to generate the initial momentum

$P(0)$). Conservation of energy is not violated since after the bounce, internal energy remains within the rod. This suggests an adjustment of the definition of COR based on translational energy $\mathcal{E}_h$ which we propose next.

4.2 Energy coefficient of restitution

Since the internal energy $\mathcal{E}_z$ of the flexible rod does not contribute to the motion of the center of mass, we define the *energy coefficient of restitution* $e_{\mathcal{E}}$ as the square root of the ratio of the energies $\mathcal{E}_h$ after, and before the impact:

$$e_{\mathcal{E}} = \left(\frac{\mathcal{E}_h(t_b)}{\mathcal{E}_h(0)}\right)^{\frac{1}{2}}. \tag{4.71}$$

The undamped case $r = 0$: From (3.66) and Theorem 2

$$\mathcal{E}_h(0) = \frac{\mu^2 L}{2} = \mathcal{E}_{tot}, \qquad \mathcal{E}_h(t_b) = \begin{cases} \frac{L\mu^2(3\mu^2 - 4\mu\mu_0 + 3\mu_0^2)}{6\mu_0^2}, & 0 \leqslant \mu < \mu_0, \\ \frac{L}{2}(\mu^2 - \frac{\mu_0^2}{3}), & \mu \geqslant \mu_0. \end{cases}$$

Thus,

$$e_{\mathcal{E}}^2 = \frac{\mathcal{E}_h(t_b)}{\mathcal{E}_h(0)} = \begin{cases} \frac{3\mu^2 - 4\mu\mu_0 + 3\mu_0^2}{3\mu_0^2}, & 0 \leqslant \mu < \mu_0, \\ 1 - \frac{\mu_0^2}{3\mu^2}, & \mu \geqslant \mu_0. \end{cases} \tag{4.72}$$

In fact, a typical graph of $e_{\mathcal{E}}^2 = \frac{\mathcal{E}_h(t_b)}{\mathcal{E}_{tot}}$ as a function of μ is given in Fig. 3 (the upper curve). In the general undamped case ($r = 0$) we can make the following observations:

(i) $\lim_{\mu \to 0} e_{\mathcal{E}} = 1$; $\qquad \lim_{\mu \to \infty} e_{\mathcal{E}} = 1$.

(ii) $e_{\mathcal{E}}$ as a function of μ is minimized $\mu = 2\mu_0/3$.

(iii) $e_{\mathcal{E}}$ is a continuously differentiable function of μ for $\mu > 0$.

Thus the relative amount of internal energy in the bouncing elastic rod is maximized at the intermediate value $\mu = 2\mu_0/3$ and as μ increases to infinity, the impact approaches perfectly elastic.

A limitation in application of this definition of COR is that when one attempts to apply this definition to repeated bounces, subsequent initial conditions of the impact would include some internal vibrations, and hence would not be of the same form (uniform velocity) as considered here. On the other hand, for some applications it could be appropriate to assume that any internal vibrations remaining after an impact are converted to heat, or otherwise dissipated before the next impact.

The damped case $r \neq 0$: Determination of the COR (using either the momentum or energy definition) is much more complex in the damped case since all formulas involve computing the complicated stress function $\Psi_r(t)$ from (2.28). Therefore we focus on the energy COR $e_{\mathcal{E}}$.

The energy COR $e_{\mathcal{E}}$ can be computed numerically by the following steps:

1. Compute the stress function $\Psi_r(t)$ using (2.28);

2. Determine the bounce time t_b from Theorem 1. This involves finding the first root of the stress function $\Psi_r(t)$, as in Figure 1.

3. Calculate $P(t_b)$ and $h(t_b)$ from (3.38) and (3.39).

4. Calculate $e_{\mathcal{E}}$ using (4.71), $\mathcal{E}_h(0) = \mu^2 L/2$, and (3.63).

For the parameters we considered, we were able to compute $e_{\mathcal{E}}$ and related graphs using Mathematica (with about 100 time steps) in about 2 minutes computational time.

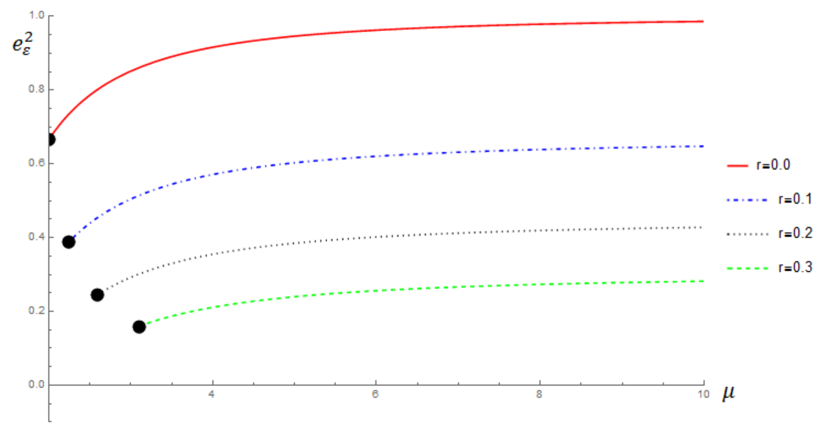

Figure 4: Plot for $e_{\mathcal{E}}^2 = \frac{\mathcal{E}_h(t_1)}{\mathcal{E}(0)}$ with $c = 1$, $L = 1$, $g = 1$, $r = 0, 0.1, 0.2, 0.3$ as a function of μ.

For the parameters considered in Figure 4, the two conditions (2.31) and (2.32) are satisfied for values of μ to the right of the black dot in each of the cases $r = 0, 0.1, 0.2, 0.3$. (These values of μ correspond to those for which $t_b = t_1$. In each case the curves continue to the left of the black dots, but are significantly more difficult to compute since t_b depends on μ and r in a more complicated way.) Thus in each case $t_b = t_1 = 2$. The red curve is the undamped case $r = 0$ and coincides with the right-most portion of the graph of the corresponding function in Figure 3.

We mention that when $r > 0$, it is possible that $\mathcal{E}_h(t_b)$ can become negative. This happens when at the time of the bounce, $h(t_b) < 0$ and the kinetic energy $P(t_b)^2/2L$ is smaller in magnitude than the drop in potential energy $|Lgh(t_b)|$; see eq. (3.63). This implies that the center of mass can never return to the initial value of $L/2$ (corresponding to $h = 0$) and thus in terms of the center of mass, there is not really a “bounce”. Therefore we leave $e_{\mathcal{E}}$ undefined in these cases.

In the case $r = 0$ we noted earlier that $\lim_{\mu\to\infty} e_{\mathcal{E}} = 1$. For $r > 0$ however the graph suggests a different limit as μ tends to infinity. In order to numerically investigate this limiting behavior more systematically, we note that

$$e_{\mathcal{E}}^2 = \frac{\mathcal{E}_h(t_b)}{\mathcal{E}(t_b)} \cdot \frac{\mathcal{E}(t_b)}{\mathcal{E}(0)}. \tag{4.73}$$

The quantity $\frac{\mathcal{E}_h(t_b)}{\mathcal{E}(t_b)}$ is the ratio of translational energy to total energy at time t_b, and can be viewed as a form of COR that is does not depend (directly) on the viscous damping.

The second is a ratio of energy at time t_b to the initial energy, hence is directly related to the decay rate of energy.

In order to analyze the terms $\frac{\mathcal{E}_h(t_b)}{\mathcal{E}(t_b)}$ and $\frac{\mathcal{E}(t_b)}{\mathcal{E}(0)}$ separately, it is necessary to compute $\mathcal{E}(t_b)$. Unfortunately there is no simple way to compute this and one must directly compute $\mathcal{E}(t_b)$ from (3.54) by computing $v_t(x, t_b)$ and $v_x(x, t_b)$ for $0 < x < L$. This computation is described in the Appendix.

The ratios $\mathcal{E}_h(t_1)/\mathcal{E}(t_1)$ and $\mathcal{E}(t_1)/\mathcal{E}(0)$ versus μ are graphed separately in Figures 5 and 6 below. We picked the same parameter values that were used in Figure 4; i.e., $g = 1.0$, $L = 1.0$, $c = 1.0$. The four curves correspond to the r values as 0.0, 0.1, 0.2 and 0.3. The values of μ changes from 3.2 to 12.5.

The graphs are linear interpolations of data based on 20 time steps. (This computation took hours to run, so we did not attempt a finer time step.)

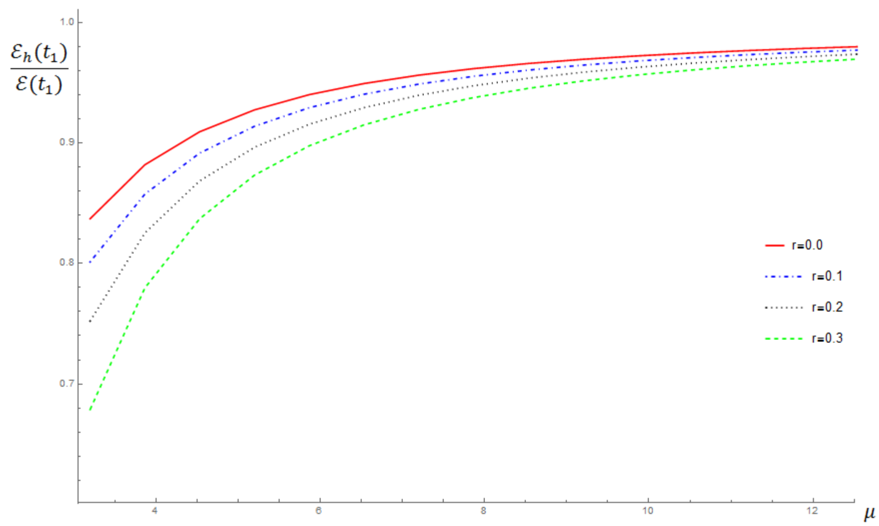

Figure 5: Plot for $\mathcal{E}_h(t_1)/\mathcal{E}(t_1)$ when $c = 1.0$, $L = 1.0$, $g = 1.0$ change with μ.

Figure 5 indicates a very similar behavior with respect to μ of the ratio $\mathcal{E}_h(t_1)/\mathcal{E}(t_1)$ compared to the undamped case, where energy is conserved, and hence $\mathcal{E}_h(t_1)/\mathcal{E}(t_1) = \mathcal{E}_h(t_1)/\mathcal{E}(0) = e_{\mathcal{E}}^2$. Since $\lim_{\mu\to\infty} e_{\mathcal{E}} = 1$. Figure 5 suggests that

$$\lim_{\mu\to\infty} \frac{\mathcal{E}_h(t_1)}{\mathcal{E}(t_1)} = 1. \tag{4.74}$$

Figure 6 suggests that the ratios $\mathcal{E}(t_1)/\mathcal{E}(0)$ are nearly constant functions of μ for large values of μ. This nearly constant value varies with respect to the damping r in a way that is related to the behavior of the decay rate of the Fourier series solution corresponding to the given initial data. This involves infinitely many modes since the initial data does not correspond to a finite combination of eigenfunctions for boundary conditions $v(0, t) = 0$, $v_x(L, t) = 0$. However the energy decay in (3.55) suggests that the ratios $\mathcal{E}(t_1)/\mathcal{E}(0)$ might be proportionate to e^{-2rt_b}. This suggests investigating the quantity $\frac{\mathcal{E}(t_1)/\mathcal{E}(0)}{e^{-2rt_1}}$ which is graphed in Figure 7.

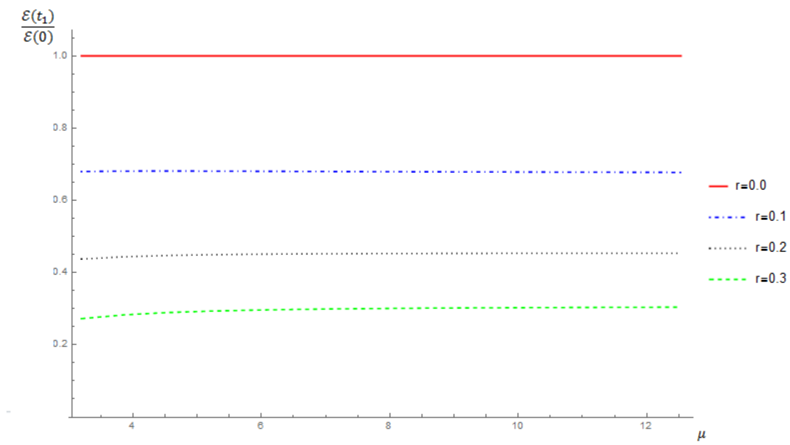

Figure 6: Plot for $\mathcal{E}(t_1)/\mathcal{E}(0)$ when $c = 1.0$, $L = 1.0$, $g = 1.0$ change with μ.

Figure 7 indicates that the quantity $\frac{\mathcal{E}(t_1)/\mathcal{E}(0)}{e^{-2rt_1}}$ tends to a common limit (approximately $C_0 = 1$ up to numerical error) for the different values of r considered.

Thus combining this with the previous observation in (4.74) and (4.73) suggest that

$$\lim_{\mu\to\infty} e_{\mathcal{E}} \simeq e^{-rt_b}. \tag{4.75}$$

We were able to verify this numerically for the curves in Figure 4 to within 0.001 for each curve. This required 100 time steps in the numerical integrations.

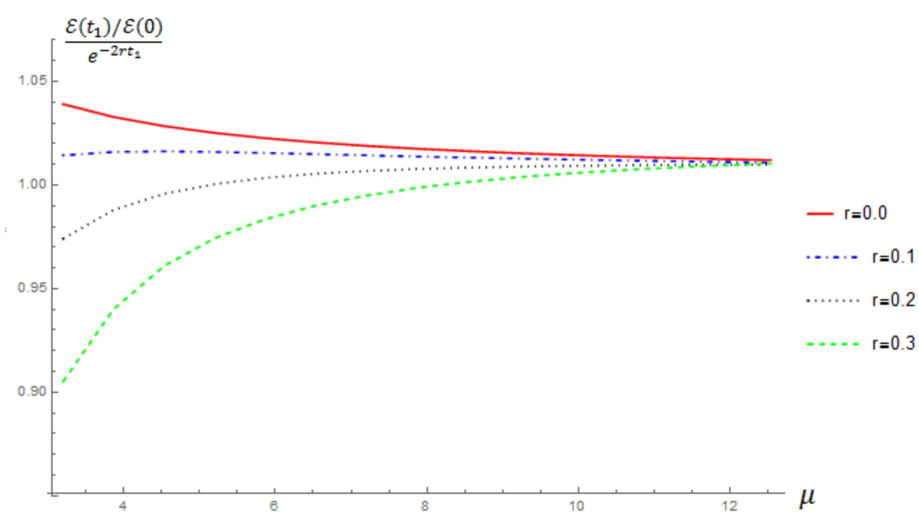

Figure 7: Plot for $\frac{\mathcal{E}(t_1)/\mathcal{E}(0)}{e^{-2rt_1}}$ when $c = 1.0$, $L = 1.0$, $g = 1.0$ change with μ.

5 Conclusions

In this paper we have analyzed the motion of a linear elastic rod with viscous damping over the duration of an impact with the ground, which is assumed to be rigid.

First, we derived an explicit solution formula (2.19) for the motion of a bouncing elastic rod during the impact. Based on this formula we were able to find an expression for the stress function $\Psi(t)$ at the bottom of the rod during the impact, and correspondingly obtain a characterization of the bounce time t_b in Theorem 1. In the undamped case ($r = 0$), there is a closed form expression for t_b described in Corollary 1, where in particular, $t_1 := 2L/c \leq t_b < 2t_1$. In the damped case we were not able to prove that Ψ must have a root (so that there is a bounce), but were able to show that if there is a root, then $t_b \geq t_1$, and moreover found examples where $t_b > 3t_1$ (see Fig. 1).

We also obtained closed form expressions (3.45), (3.46) in terms of $\Psi(t)$ and physical constants c, μ, g, L for the relative center of mass $h(t)$ and momentum $P(t)$ for the time interval $[0, t_2]$. If $r = 0$, these expressions become explicit in terms parameters c, μ, g, L; see (3.50)-(3.53).

At the time t_b, the total energy $\mathcal{E}(t)$ has an orthogonal decomposition into translational energy $\mathcal{E}_h(t)$ and vibrational energy $\mathcal{E}_z(t)$. Since $\mathcal{E}_h$ can be expressed in terms of h and P, we obtained explicit expressions in terms of $\Psi(t)$ for $\mathcal{E}_h(t)$ for $t \in [0, t_2]$. This led to a natural energy-based definition for the COR $e_{\mathcal{E}}$ defined in (4.71). With this definition, $e_{\mathcal{E}} = .9$, for example, would indicate that 81 percent of the original energy was in translational form at the end of the impact, and 19 percent was either dissipated by damping or in vibrational form. In the undamped case, $e_{\mathcal{E}}$ is given explicitly in terms of parameters c, μ, g, L in (4.72) and is graphed as a function of μ in Fig. 3.

In the damped case, the expression for $e_{\mathcal{E}}$ depends on the stress function $\Psi(t_b)$, and hence the behavior with respect to μ is more complex when bounce times need to be calculated. Figures 4 describes the behavior with respect to μ when μ is large enough so that $t_b = t_1$ (so that the computation is not difficult). Part of the value of $e_{\mathcal{E}}$ is due to damping and part is due to the ratio of vibrational energy to total energy at the end of the contact period, as indicated in (4.73). Figures 5, 6, 7 characterize, up to numerical error, the behavior with respect to μ of the decomposition (4.73) of $e_{\mathcal{E}}$. Based on these graphs, we suspect that the limiting behavior with respect to μ is described by (4.75), which at least for the examples considered, seems to be correct.

6 Acknowledgements

This research was supported in part by the Institute for Mathematics and its Applications with funds provided by the National Science Foundation. In addition, the second author was supported by the National Science Foundation under grant DMS-1312952.

7 Appendix

In this appendix, we sketch the steps that were taken to numerically compute $\mathcal{E}(t_1)$, particularly when $r \neq 0$ and $t_b = t_1$. Reviewing equation (3.54),

$$\mathcal{E}(t_1) = \frac{1}{2} \int_0^L \left(v_t(x, t_1)^2 + c^2 v_x(x, t_1)^2 \right) \, dx + Lgh(t_1).$$

$h(t_1)$ can be calculated using (3.38) and (3.39) as shown in Section 3.1. Alternatively, (3.34) can be used once $v_t(x, t_1)$ has been computed numerically. Then again use (3.39) to get $h(t_1)$. We need to compute $v_t(x,t_1)$ and $v_x(x,t_1)$. The idea is to apply equations (2.22), (2.23) and (2.24) with $v(x,t) = e^{-rt}w(x,t)$, $\phi^e(y) = -\mu^e(y)$ and $h^e(y,t-\tau) = -g^e(y)e^{r(t-\tau)}$.

Thus, $v_t(x,t_1)$ and $v_x(x,t_1)$ can be computed from $w(x,t_1)$, $w_t(x,t_1)$ and $w_x(x,t_1)$ as below:

$$\begin{aligned} v_t(x,t_1) &= -re^{-rt_1}w(x,t_1) + e^{-rt_1}w_t(x,t_1), \\ v_x(x,t_1) &= e^{-rt_1}w_x(x,t_1). \end{aligned}$$

The integrands for the terms $w(x,t_1)$, $w_t(x,t_1)$ and $w_x(x,t_1)$ have discontinuities along characteristic lines $ct = \pm(x-2kL), k \in \mathbb{Z}$. Consequently some care should be taken to evaluate the integrals correctly in the separate regions, which are defined by the characteristics, see Fig. 8. For example, in order to compute $w_t(x,t_1)$, after using the definition of the extended functions μ^e and g^e, and recall that $\lambda = r/c$ and $s(t,r) = \sqrt{c^2t^2 - r^2}$, (2.23) becomes the following,

$$\begin{aligned} w_t(x,t_1) &= \frac{1}{2c}\Bigg(c^2t_1\mu\lambda\int_{x-ct_1}^{0}\frac{I_1(\lambda s(t_1,x-y))}{s(t_1,x-y)}\,dy - c^2t_1\mu\lambda\int_0^{2L}\frac{I_1(\lambda s(t_1,x-y))}{s(t_1,x-y)}\,dy \\ &+ c^2t_1\mu\lambda\int_{2L}^{x+ct_1}\frac{I_1(\lambda s(t_1,x-y))}{s(t_1,x-y)}\,dy + 2c\mu \\ &+ g\Big(\int_{x-ct_1}^{0} I_0(\lambda s(t_1,x-y))s(t_1,x-y)\,dy - \int_0^{2L} I_0(\lambda s(t_1,x-y))s(t_1,x-y)\,dy \\ &+ \int_{2L}^{x+ct_1} I_0(\lambda s(t_1,x-y))s(t_1,x-y)\,dy\Big) \\ &+ r\int_0^{t_1}\int_{x-c\tau}^{x+c\tau} I_0(\lambda s(\tau,x-y))(-g^e(y)e^{r(t_1-\tau)})\,dyd\tau\Bigg). \end{aligned} \tag{7.76}$$

We handle the last double integral as follows. Given a point (x,t_1), where $x \in (0,L)$, the region of integration is the region in Fig. 8 determined by characteristic lines emanating from point (x,t_1). We write this integral as a sum of three integrals, based on their region of integration. In Fig. 8, the purple regions correspond to $g^e(x) = -g$, while the green area corresponds to $g^e(x) = g$. Taking this geometry into consideration, the last term can be written as

$$\begin{aligned} & r\int_0^t\int_{x-c\tau}^{x+c\tau} I_0(\lambda s(\tau,x-y))(-g^e(y)e^{r(t-\tau)})\,dyd\tau \\ =\ & 2\Big(-r\int_{x-ct_1}^{0}\int_0^{t_1+\frac{y-x}{c}}(-g)I_0(\lambda s(t_1-\tau,x-y))e^{r\tau}\,d\tau dy\Big) \\ +\ & \Big(-r\int_0^{t_1}\int_{x-c(t_1-\tau)}^{x+c(t_1-\tau)}(g)I_0(\lambda s(t_1-\tau,x-y))e^{r\tau}\,dyd\tau\Big) \\ +\ & 2\Big(-r\int_{2L}^{x+ct_1}\int_0^{t_1-\frac{y-x}{c}}(-g)I_0(\lambda s(t_1-\tau,x-y))e^{r\tau}\,d\tau dy\Big). \end{aligned}$$

Similar explicit expressions for $w(x,t_1)$ and $w_x(x,t_1)$ can likewise be written down. Therefore, $\mathcal{E}(t_1)$ can be expressed in terms of integrals that can be computed numerically using Mathematica.

As a benchmark, we computed $\mathcal{E}(t_1)$ the way in the conservative case $r = 0$, and obtained the red curves in Fig. 5, 6, 7, which has about 1% error using Mathematica 10.3.

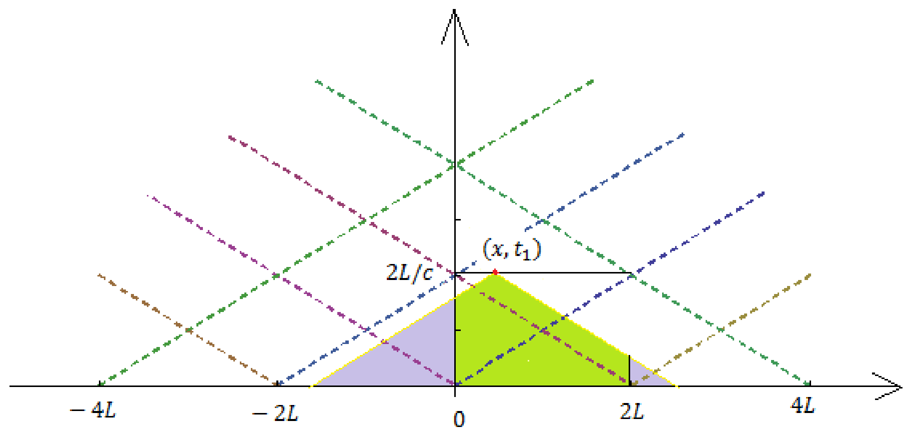

Figure 8: Integration regions A, B and C.

References

[1] J. Ahn, *A vibrating string with dynamic frictionless impact*, Applied numerical mathematics, 57 (2007), pp. 861–884.

[2] J. Ahn and D. E. Stewart, *Dynamic frictionless contact in linear viscoelasticity*, IMA journal of numerical analysis, 29 (2009), pp. 43–71.

[3] F. Ammar-Khodja, S. Micu, and A. Münch, *Controllability of a string submitted to unilateral constraint*, in Annales de l'Institut Henri Poincare (C) Non Linear Analysis, vol. 27, Elsevier, 2010, pp. 1097–1119.

[4] R. Cross, *Mechanics of swinging a bat*, American Journal of Physics, 77 (2009), pp. 36–43.

[5] H. Hertz, *Über die berührung fester elastischer körper*, (1882).

[6] Y.-B. Jia, M. Mason, and M. Erdmann, *A state transition diagram for simultaneous collisions with application in billiard shooting*, in Algorithmic Foundation of Robotics VIII, Springer, 2009, pp. 135–150.

[7] F. John, *Partial differential equations, volume 1 of applied mathematical sciences*, 1982.

[8] K. L. Johnson and K. L. Johnson, *Contact mechanics*, Cambridge university press, 1987.

[9] G. Lebeau and M. Schatzman, *A wave problem in a half-space with a unilateral constraint at the boundary*, Journal of differential equations, 53 (1984), pp. 309–361.

[10] P. Lipscombe and S. Pellegrino, *Free rocking of prismatic blocks*, Journal of engineering mechanics, 119 (1993), pp. 1387–1410.

[11] S. Liu, L. Wu, and Z. Lu, *Impact dynamics and control of a flexible dual-arm space robot capturing an object*, Applied mathematics and computation, 185 (2007), pp. 1149–1159.

[12] A. E. H. Love, *A treatise on the mathematical theory of elasticity*, vol. 1, Cambridge University Press, 2013.

[13] J. Rivera and H. P. Oquendo, *Exponential decay for a contact problem with local damping*, FUNKCIALAJ EKVACIOJ SERIO INTERNACIA, 42 (1999), pp. 371–388.

[14] P. Shi, *The restitution coefficient for a linear elastic rod*, Mathematical and computer modelling, 28 (1998), pp. 427–435.

[15] ——, *Simulation of impact involving an elastic rod*, Computer methods in applied mechanics and engineering, 151 (1998), pp. 497–499.

[16] D. E. Stewart, *Rigid-body dynamics with friction and impact*, SIAM review, 42 (2000), pp. 3–39.

[17] W. J. Stronge, *Impact mechanics*, Cambridge university press, 2004.

[18] I. D. Walker, *Impact configurations and measures for kinematically redundant and multiple armed robot systems*, IEEE transactions on robotics and automation, 10 (1994), pp. 670–683.

[19] F. Wang, H. Lin, and Y.-B. Jia, *Computational modeling of n-body collisions*, in Intelligent Robots and Systems (IROS), 2015 IEEE/RSJ International Conference on, IEEE, 2015, pp. 5376–5381.

[20] Y. Wang and M. Mason, *Modeling impact dynamics for robotic operations*, in Robotics and Automation. Proceedings. 1987 IEEE International Conference on, vol. 4, IEEE, 1987, pp. 678–685.

[21] H. Zhang, B. Brogliato, and C. Liu, *Dynamics of planar rocking-blocks with coulomb friction and unilateral constraints: comparisons between experimental and numerical data*, Multibody System Dynamics, 32 (2014), pp. 1–25.